# Testing extreme warming and geographical heterogeneity

María Dolores Gadea Rivas[a], Jesus Gonzalo[b] and Jose Olmo[c,d]

[a]Department of Applied Economics, University of Zaragoza. Gran Vía, 4, 50005 Zaragoza (Spain); [b]Department of Economics, University Carlos III, Madrid 126 28903 Getafe (Spain); [c]Department of Economic Analysis, University of Zaragoza. Gran Vía, 4, 50005 Zaragoza (Spain);[d]Department of Economics, University of Southampton, Highfield Campus, SO17 1BJ, Southampton (UK).

**ARTICLE HISTORY**
Compiled April 15, 2025

**ABSTRACT**
Extreme climate events represent a critical climate risk and a global challenge. Understanding the heterogeneity in worldwide temperatures is crucial for predicting future climate change dynamics and guiding effective policy responses. This paper addresses both issues by analyzing the presence of trends in the tail decay of the realized distribution of annual temperatures for eight regions spanning the globe over the period 1960 to 2022. Our empirical findings reveal that extreme warming exhibits heterogeneity across regions and seasons, with a pronounced distinction between the Northern and Southern hemispheres. Importantly, extreme warming predominantly occurs in both hemispheres during the period from June to September.

**KEYWORDS**
extreme value theory, Hill estimator, global warming, tail behavior, trend detection

## 1. Introduction

Climate indeed encompasses multiple dimensions, but those that carry the most weight pose risky consequences on the planet—known as climate risks. Among the primary contributors to climate risk are extreme temperatures, which often lead to severe weather events. Climate change exacerbates this phenomenon, resulting in more frequent and intense heat waves, droughts, storms, and other extreme weather occurrences. These events pose significant risks to various aspects of human life, including health, infrastructure, agriculture, and ecosystems. For instance, extreme temperatures can directly impact human health, leading to heat-related illnesses and fatalities. They can also influence human behavior, affecting outdoor activities, energy consumption, and migration patterns. Furthermore, extreme weather events can damage critical infrastructure, disrupt agricultural systems, and threaten the stability of ecosystems, with far-reaching implications for biodiversity and ecosystem services. Therefore, understanding and mitigating the risks associated with extreme temperatures and related weather events are essential for ensuring the well-being of humans and the environment in the face of ongoing climate change. The IPCC Sixth Assessment Report comprehensively summarizes the academic work addressing these issues (IPCC, 2022a).

Jose Olmo. Email: joseolmo@unizar.es

Addressing these climate risks is essential for safeguarding the planet's future and its inhabitants. Growing empirical evidence of a gradual warming trend in global mean temperature, as demonstrated by Hansen and Lebedeff (1987, 1988), has heightened awareness of human-induced climate change through pollution and carbon emissions. However, the primary impacts of climate change on society stem from extreme events, reflecting the inherent variability of climate. Nevertheless, attempts to quantify the nature of such relationships have been relatively scarce (Mearns et al., 1984; Wigley, 1988). Katz and Brown (1992) represent one of the pioneering efforts to study the relative sensitivity of extreme events to the mean and variability (location and scale parameters) of climate. In their seminal work, they find that extreme events are susceptible to climate variability compared to their average, and this sensitivity increases with the extremity of the event. To achieve this, these authors consider a model in which climate change involves a combination of two different statistical operations represented by changes in location or scale parameters.

Although climate extremes are, by definition, rare events, climate change has resulted in changes in the occurrence of extreme events (Easterling et al., 2000; Seneviratne et al., 2012). Climate extremes can result from external forces of the climate system, such as increasing greenhouse gases, natural variability, or a combination of the two. Recent work by Ballester et al. (2010), Katz (2010), Zwiers et al. (2011), and Easterling et al. (2016), amongst others, discuss changes in climatic extremes over time and focus on the human effect with both observational data and data from climate models. Thus, in the past decade, climate extremes have steadily become a focus of detection and attribution studies[1].

Early studies of climate extremes considered climate data to be homogeneous. In these studies, extremes result from variations and trends in central statistics, such as the mean, variance, or skewness. For example, Ballester et al. (2010) find that changes in European temperature extremes can be predicted from changes in the distribution of central statistics. From a statistical point of view, these studies accommodate the presence of time trends in such statistics. These analyses are further extended by Gadea and Gonzalo (2020, 2025, referred to as GG2020 and GG2025 hereafter) that explore changes in distributional characteristics, with particular emphasis on the quantile process, and investigate the presence of time trends amplifying the impact and severity of climate change. Their findings suggest climate change evidence extends beyond mean temperatures, indicating that warming is a global phenomenon. These authors observe heterogeneous occurrences of global warming, manifesting at different speeds across quantiles and regions. GG2020 mainly identifies an increasing trend in all distributional characteristics (both time series and cross-sectional) when analyzing temperatures worldwide from all available weather stations. The trend is notably more prominent in the lower quantiles than the mean, median, and upper quantiles. Furthermore, a negative trend in dispersion measures such as the standard deviation and interquartile range indicates that lower temperatures approach the median faster than higher temperatures.

Recent literature extends these analyses of extreme events based on central statistics by focusing on variations in the distribution of the block maxima over time. This literature shows that it is straightforward to introduce trends into the parameters of the Generalized Extreme Value distribution (GEV) used for modeling the block maxima (e.g., a linear trend in the location parameter and/or in the logarithm of the scale

[1]Detection is the identification of a statistically significant change in the extreme values of a climate variable over some time, whereas attribution studies the likely causes (especially, human-related greenhouse gas emissions) of such events.

parameter), see Gumbel (1941, 1958) for theoretical results on the distribution of the block maxima, Coles (2001) for an introduction to statistical modeling of extreme values, and Katz et al. (2002), Zwiers et al. (2011) and Easterling et al. (2016) for the analysis of climate variables. More modern extreme value theory attempts to use more of the available information about the upper tail of a distribution than just the block maxima. In this setting, information about the $k$ largest extreme observations is relevant for understanding the magnitude of the extreme event. The distribution function for modeling these events is the Generalized Pareto. The tail (shape) parameter that determines the tail decay and, hence, the likelihood of extreme events has the same interpretation as for the block maxima; see Embrechts, Kluppelberg, and Mikosch (1997) for a review of extreme value theory and Katz (2010) for the application of these models for the statistics of extremes in climate change.

Building upon these previous studies on the dynamics of centrality measures such as the mean and variance and distributional characteristics such as the quantile process for the analysis of climate change, our first contribution is to delve deeper into the dynamics of extreme temperatures. There is a strong link between rising global temperatures and the increased frequency and intensity of extreme climate events such as wildfires, droughts, and floods. In this paper we only show how to detect the evolution of extreme temperature events. Specifically, we focus on the tail parameter, which comprehensively characterizes distribution behavior in the tails. Our objective is to ascertain whether the increased likelihood of recent extreme events in climate variables stems from positive trends in distributional characteristics such as the mean and the quantile process, as observed in GG2020 and GG2025, or from the rise in extreme temperatures themselves. To accomplish this, we adapt the tests developed in GG2020 and GG2025 to statistically assess the presence of time trends of unknown form in the tail parameter.

The conclusions of our empirical study depend heavily on the quality of the tail parameter estimates. To the best of our knowledge, the effect of estimating the tail parameters using data exhibiting location shifts has received limited attention. Whereas there is a specialized literature in statistics of extremes that has studied the impact of location shifts in the finite-sample and asymptotic properties of standard estimators of the tail parameter, see Fraga Alves (2001), Aban and Meerschaert (2001), and Ling et al (2007a, 2007b, 2012), among a few others, suitable corrections are generally not considered when applying extreme value theory esimators to real data exhibiting location and scale effects. Thus, our second contribution is to examine the finite-sample impact of estimating the tail parameter directly from data drawn from location-scale processes and compare the quality of these estimates of the tail parameter with those obtained from suitable corrections that account for location shifts. In particular, we consider transformations of the original data given by demeaning the observations. This approach can be interpreted as an alternative to the choice of intermediate order statistics proposed in Fraga Alves (2001) and subsequent literature. We will focus on popular estimators of the tail parameter such as the Hill (1975) estimator and regression-based estimators, see Gabaix and Ibragimov (2012), with further references in Rosen and Resnick (1980), Gabaix (1999), and Gabaix and Ioannides (2004), among others. These estimators are all invariant to scale effects but are affected in finite samples by location effects. This is a necessary step in our empirical application in order to be able to identify the source of dynamics in extreme temperatures and determine whether these dynamics are due to location shifts of the parent distribution of temperatures over time, to increases in the likelihood of extreme events (heavier tails) once location effects are controlled for, or both. To achieve this, we present a thorough

simulation study that compares the finite-sample performance of different versions of the Hill and regression-based estimators of the tail parameter constructed from raw and demeaned data generated by the family of Student-t distributions with different degrees of freedom. The empirical results provide evidence of finite-sample differences in the estimation of the tail parameter, even for very large sample sizes. The estimators of the tail parameter obtained from the order statistics of demeaned sequences outperform those obtained from raw sequences if the location parameter is large in magnitude and for heavy-tailed distributions.

Our third and main contribution is to assess the heterogeneity in extreme temperatures across regions. We expand on the work of GG2025, which examines different regions separately and introduces the concept of geographic heterogeneity in the warming process. These authors define four distinct types of warming based on the trend exhibited by the quantile process[2]. GG2025 does not investigate trends in the dynamics of extreme temperatures below the 5th quantile and beyond the 95th quantile. As a result, their conclusions may only partially capture warming trends in extreme temperatures beyond those observed for distributional characteristics such as the mean, median, or fixed quantiles. This is, for example, the case for the Antarctic region. Our empirical application reveals different warming patterns depending on whether we focus on the dynamics of the quantile process or the dynamics of the tail behavior. The current study aims to address these gaps in research by examining trend dynamics in extreme temperatures, providing a comprehensive understanding of climate change impacts on the tails of temperature distributions over time.

Heterogeneity is captured through the analysis of eight distinct regions (the Antarctic Polar Circle, the Arctic Polar Circle, Africa, Asia, Australia, Europe, North America, and South America) covering the globe from 1960 to 2022. Using a panel of monthly temperatures from a large cross-section of weather stations, we estimate the tail parameters from cross-sectional realized distributions applied to each of these regions and obtain a time series of tail parameter estimates for each tail of the distribution. By doing so, we not only uncover the presence of heavy-tailed temperature distributions driving extreme weather events but also gauge the extent of extreme warming over time and across seasons. Thus, some regions may currently face a lower likelihood of extreme temperatures than others but at the same time reveal stronger dynamics of the tail parameter that predict more severe extreme warming patterns in the near term. Three salient patterns emerge from our empirical analysis of heterogeneity in the warming process of extreme temperatures across regions and over time:

i) North America, Asia and Antarctica: Extreme warming affects the right tail of the temperature distribution, with extreme temperatures steadily increasing in recent years. This increase is above and beyond the expected increase implied by a uniform positive shift to the whole distribution of temperatures. In contrast, extreme temperatures in the left tail do not show evidence of warming.
ii) Europe, Africa and the Arctic Polar Circle: Our empirical results do not indicate evidence of warming in the extremes despite the steady increase in the quantiles of temperature distributions found in GG2020.
iii) Southern Hemisphere - South America and Australia: Extreme warming affects the left tail of the temperature distribution, with extreme temperatures steadily increasing in recent years. This increase is above and beyond the expected in-

[2]Climate change is not a uniform phenomenon. This assertion is already well known in the climate literature (IPCC, 2021, 2022a, 2022b), but the GG2025 approach is more appropriate since each distributional characteristic is converted into a time series object.

crease implied by a uniform positive shift to the whole distribution of temperatures. In contrast, extreme temperatures in the right tail do not experiment evidence of warming.

The study of temperature dynamics is usually carried out at the station level or grid anomalies, which entails the application of univariate time series models. In this paper, we depart from these conventional analyses by considering the mean monthly temperature as the unit of study. The mean monthly temperature is computed as the average between the monthly maximum and minimum temperatures. This approach, also proposed by Jones et al. (2012) and utilized in the Climatic Research Unit (University of East Anglia) databases, allows us to incorporate information from both the maximum and minimum temperatures into a single unit of measure. This provides smoother details about the temperature dynamics than observations based solely on the maximum or minimum temperatures obtained separately. The second departure from the literature lies in considering cross-sectional information to construct the realized distribution of annual temperatures. Leveraging the concept of realized measures, we consider average monthly data obtained from the cross section of all available weather stations in a given year to estimate what we term as the realized distribution of annual temperatures for a geographical region in a given year. By adopting this approach, we capture the cross-sectional dispersion of temperatures and seasonal effects. In contrast to GG2020 and GG2025, which utilize the same construction of the distribution of annual temperatures to examine the dynamics of centrality and dispersion measures, our current analysis shifts focus towards modeling the dynamics of the tail decay, and, consequently, the likelihood of extreme events.

The paper is structured as follows. Section 2 reviews the primary results of Extreme Value Theory (EVT) and tail behavior under Pareto-type approximations. Section 3 introduces several definitions of warming in the extremes and discusses various tests to detect the presence of trends of general form in distributional characteristics. Section 4 reviews popular estimators of the tail parameter such as the Hill and regression-based estimators and presents a simulation exercise that assesses the finite-sample discrepancies between versions of these estimators constructed from sequences of order statistics obtained from raw and demeaned data. Section 5 presents an empirical application to a panel of monthly temperatures, analyzing the dynamics of the tail parameter in both tails of the realized distribution of annual temperatures. We divide the globe into eight regions and construct time series estimates of the tail parameters obtained from cross-sectional data on temperatures recorded from weather stations. We analyze the warming patterns of extreme temperatures in both tails and classify the regions according to their warming type. Section 6 concludes.

## 2. Background theory

This section introduces some background theory required to understand the models and methods introduced below.

### 2.1. *Basic results on extreme value theory*

Extreme Value Theory (EVT) studies the limiting distribution of the standardized maxima (and minima) of a random sample $\{X_i\}_{i=1}^n$ of size $n$. Let $M_n = \max\{X_1, \ldots, X_n\}$ be the sample maximum and let $F(x)$ denote the probability law

generating such observations. Gnedenko (1943) and de Haan (1976) were the first authors to characterize the limiting distribution of the standardized maximum for independent and identically distributed (iid) data. Under these assumptions, there are normalizing sequences $a_n$ and $b_n$ such that $P\{a_n^{-1}(M_n - b_n) \leq x\} \to G(x)$, as $n \to \infty$, with $G(x) = e^{-\tau(x)}$. This result is further refined depending on the maximum domain of attraction of the parent distribution $F(x)$. Thus, $\tau(x)$ can only be of three forms: (i) Type I (Gumbel): $\tau(x) = e^{-x}$ for $x \in (-\infty, \infty)$; (ii) Type II (Fréchet): $\tau(x) = x^{-\xi}$ for $x > 0$ and $\xi > 0$; (iii) Type III (Weibull): $\tau(x) = -(-x)^{\xi}$ for $x < 0$ and $\xi < 0$. The three types of extreme value distributions can be expressed in the so-called Generalized Extreme Value Distribution, first proposed by von Mises (1936), and given by $G(x) = e^{-\tau(x)}$ with $\tau(x) = \left(1 + \frac{1}{\xi}x\right)^{-\xi}$ for $\xi \neq 0$, and $\tau(x) = e^{-x}$ for $\xi = 0$. The distribution of the standardized maximum is fully characterized by the shape parameter $\xi$. This parameter is the inverse of the so-called tail index used in the EVT literature. For notational convenience, we will hereafter use the expression *tail parameter* to refer to the shape parameter $\xi$ introduced above and *tail index* $\psi$ to its inverse.

The above asymptotic results for the distribution of the maximum for *iid* data also implies the following approximation $n(1 - F(a_n x + b_n)) \to \tau(x)$, for $a_n$ and $b_n$ suitable sequences and $x$ sufficiently large[3]. In this setting, an extreme observation is characterized by a value $x$ sufficiently large in magnitude to be in the tail of the parent distribution $F(\cdot)$. Importantly, the function $\tau(x)$ and, in particular, the tail parameter $\xi$ determine the behavior of the distribution in the right tail and, hence, the probability of extreme events. Broadly speaking, a positive value of the tail parameter indicates a polynomial decay of the distribution in the tail and, hence, the presence of heavy tails. More formally, a heavy-tailed distribution is defined as a distribution function $F(x)$ such that

$$1 - F(x) = x^{-\xi}\mathcal{L}(x), \tag{1}$$

where $\mathcal{L}(x)$ is a slowly varying functon satisfying $\lim_{t\to\infty} \frac{\mathcal{L}(tx)}{\mathcal{L}(t)} = 1$ for $x > 1$. Values of $\xi$ in the interval $(0, 20)$ are usually identified with the presence of heavy tails and the scenario $\xi > 20$ corresponds to a tail with exponential decay. The case $\xi < 2$ corresponds to very heavy tailed distribution functions characterized by infinite variance, and $\xi < 1$ by a distribution function with no mean. Interestingly, for the Student-t family of distributions the tail parameter coincides with the degrees of freedom coefficient.

**Remark 1:** The above asymptotic results show that location-scale transformations of the parent distribution $F(x)$ do not affect its tail behavior. Location and scale parameters are incorporated in the asymptotic results through suitable transformations of the sequences $a_n$ and $b_n$.

**Remark 2:** Let $Y = \mu + \sigma X$ denote a location ($\mu$) - scale ($\sigma$) transformation of the standard random variable $X$. Let $F_x$ be the distribution function of $X$ that satisfies

[3]Similar asymptotic results are obtained under weak dependence in the extreme observations. In this case the asymptotic distribution depends on an additional parameter, extremal index, that measures the degree of clustering in the extremes, see Leadbetter, Lindgren and Rootzén (1983), O'Brien (1987), and Hsing (1993) for a review of extreme value theory for weakly dependent stationary sequences.

condition (1). It follows that

$$1 - F_y(y) = 1 - F_x\left(\frac{y-\mu}{\sigma}\right) = \left(\frac{y-\mu}{\sigma}\right)^{-\xi} \mathcal{L}(x), \tag{2}$$

for $x = (y-\mu)/\sigma > 1$. The tail of the parent distribution $F_y$ can be approximated by the tail of a Pareto distribution for $y$ sufficiently large.

Remark 2 shows that the probability of an extreme event in location-scale models is completely characterized by the location and scale parameters $\mu$ and $\sigma$, respectively, and the tail parameter $\xi$. To show this, let $x > 1$ denote an extreme positive event associated to the random variable $X$. Following expression (1), the probability of the extreme event is $P\{X > x\} \approx x^{-\xi^R}$, with $\xi^R$ the tail parameter driving the behavior in the right tail. Under a location-scale transformation of the random variable the probability of the extreme event is $P\{Y > y\} \approx \left(\frac{y-\mu}{\sigma}\right)^{-\xi^R}$. The probability increases with the location and scale parameters and decreases with the tail parameter $\xi^R$. In contrast, the probability of an extreme event of same magnitude in the left tail is $P\{X \leq x\} \approx (-x)^{-\xi^L}$, with $x < 0$, and $\xi^L$ denoting the tail parameter driving the behavior in the left tail. Similarly, for the location-scale transformation, it follows that $P\{Y \leq y\} \approx \left(-\frac{y-\mu}{\sigma}\right)^{-\xi^L}$, with $y < \mu$. In contrast to the right tail, for the left tail the probability of extreme events decreases as the location parameter rises. The relation between the other two parameters (scale and tail behavior) and the probability of positive extremes is the same as for the right tail.

**Remark 3:** More formally, we follow the literature on Extreme Value Theory, see Pickands (1975) and de Haan (1976), and define an extreme event as an observation in the tails of the distribution of the parent distribution $F(\cdot)$. Each tail is defined by a cut-off point beyond which the tail observations asymptotically follow a Generalized Pareto distribution. This property of extreme observations, also known as Pickands theorem, was first used by Gonzalo and Olmo (2004) to define the sequence of extreme values for very general classes of distribution functions.

In what follows, we abstract from specific choices of the cut-off point that defines the tail of the temperatures distribution and simply characterize the behavior of extreme temperatures through the value and dynamics of the tail parameter in each tail.

## 3. Modeling dynamics in extreme temperatures

The above results modeling the probability of extreme events can be adapted to modeling the dynamics of extreme temperatures over time. In GG2020, temperature is viewed as a functional stochastic process $X = (X_t(\omega), t \in T)$, where $T$ is an interval in $\mathbb{R}$ defined in a probability space $(\Omega, \Im, P)$. In contrast to these authors, which focus on modeling a variety of distributional characteristics such as the mean, median, and quantile processes, our interest in this paper lies in modeling the tail behavior of the sequence of distribution functions $(F_1(\omega), \ldots, F_T(\omega))$. This is represented by the sequence of tail parameters $(\xi_1(\omega), \ldots, \xi_T(\omega))$. These distributional characteristics can be considered time series objects, allowing us to apply all the econometric tools developed in the time series literature to $\xi_t(\omega)$. Furthermore, throughout this paper, similar

to the assumptions made in Park and Qian (2012) and Chang et al. (2016), we assume that in each period $t$, there are sufficient temporal or cross-sectional observations ($n \to \infty$) for these characteristics to be estimated consistently.

GG2020 define warming as the existence of an increasing trend in certain characteristics measuring the central tendency or position (quantiles) of the temperature distribution. GG2025 introduce four characterizations of the warming process depending on the relative speed across quantiles $q_t(\tau)$, with $\tau \in (0,1)$, of the location parameters associated to each $\tau$ driving their dynamics. More formally,

**Definition 1 (Typology of warming process):**

- **W0**: There is no trend in any of the quantiles (No warming).
- **W1**: All the location distributional characteristics have the same positive trend (dispersion does not contain a trend).
- **W2**: The Lower quantiles have a larger positive trend than the Upper quantiles (dispersion has a negative trend).
- **W3**: The Upper quantiles have a larger positive trend than the Lower quantiles (dispersion has a positive trend).

Following these characterizations of the warming process we introduce several definitions of extreme warming based on the dynamics of the tail parameter in each tail of the distribution of annual temperatures.

**Definition 2 (Extreme Warming):** We define three possible warming scenarios characterized by extreme temperatures:

- **WE0**: There is no trend in any of the tail parameters $\xi_t^L$ and $\xi_t^R$.
- **WE1**: The tail parameter $\xi_t^L$ has a positive trend.
- **WE2**: The tail parameter $\xi_t^R$ has a negative trend.

WE0 describes a scenario with no warming in extreme temperatures. The likelihood of extreme events once we control for location and scale effects remains constant over time and is characterized by the tail parameters $\xi^L$ and $\xi^R$. WE1 characterizes a scenario given by warming in extreme temperatures in the left tail of the distribution. An increase in the tail parameter over time implies a decrease in the fatness of the tail and, therefore, a smaller probability of a left tail extreme event. WE2 characterizes a scenario given by an increase in the likelihood of extreme positive temperatures over time. Interestingly, the warming scenarios $W0 - W3$ are mutually exclusive. However, our characterization of the warming process in the extremes allows for WE1 and WE2 to occur simultaneously, as these phenomena refer to different tails. Thus, we can observe two types of warming in the extremes for the same region.

The following definition introduces an empirically testable characterization of extreme warming based on the presence of trends in the tail parameters.

**Definition 3:** The tail parameter $\xi_t$ obtained from the sequence of distribution functions $F_t(\cdot)$ contains a trend if in the least squares (LS) regression,

$$\xi_t = \alpha + \beta t + u_t, \ t = 1, \dots T, \tag{3}$$

the hypothesis $H_0 : \beta = 0$ is rejected. This hypothesis can be tailored to specify if the trend is positive or negative. Thus,

(a) for $\xi_t^L$, there is evidence of warming if $\beta > 0$ such that the hypothesis of interest is $H_{0TL} : \beta \leq 0$ against $H_{ATL} : \beta > 0$;
(a) for $\xi_t^R$, there is evidence of warming if $\beta < 0$ such that the hypothesis of interest is $H_{0TR} : \beta \geq 0$ against $H_{ATR} : \beta < 0$.

GG2020 shows for the analysis of distributional centrality and dispersion measures that a simple t-test for the hypothesis $\beta = 0$ is able to detect most of the existing deterministic trends (polynomial, logarithmic, exponential, etc) and also the trends generated by any of the three standard persistent processes considered in the literature: (i) fractional or long-memory models ($1/2 < d < 3/2$); (ii) near-unit-root AR models; and (iii) local-level models. Furthermore, if regression (3) is the true data generating process, with $u_t$ a stationary process, then the distribution of the robust HAC version of the t-test under the null hypothesis is $N(0, 1)$.

The section concludes by adapting the concept of reaction introduced in GG2025 to measure the sensitivity of tail events to shifts in the mean process. This definition is relevant for gauging increases in the likelihood of extreme temperatures that exceed those attributable to variations in mean temperatures over time.

**Definition 4:** (Tail warming reaction with respect to the mean):

(a) We say that the left tail reacts with respect to shifts in the mean process if in the following regression:

$$\xi_t^L = \alpha + \lambda^L \mu_t + u_t, \ t = 1, \dots T, \tag{4}$$

the hypothesis $H_{0RL} : \lambda^L \leq 0$ is rejected against the hypothesis $H_{ARL} : \lambda^L > 0$.
(b) We say that the right tail reacts with respect to shifts in the mean process if in the following regression:

$$\xi_t^R = \alpha + \lambda^R \mu_t + u_t, \ t = 1, \dots T, \tag{5}$$

the hypothesis $H_{0RR} : \lambda^R \geq 0$ is rejected against the hypothesis $H_{ARR} : \lambda^R < 0$.

Under the above characterizations, we say that the left tail of the distribution reacts to positive shifts in mean temperatures if it becomes thinner over time as mean temperatures increase. This indicates that both the bulk of the temperature distribution and its extremes shift to the right, resulting in a lower likelihood of very low temperatures than implied by a uniform positive shift to the whole distribution of temperatures. Conversely, we say that the right tail reacts to an increase in mean temperatures if it becomes thicker over time, indicating a higher likelihood of extreme high temperatures than implied by a uniform positive shift as the one described above.

To illustrate the phenomenon of reaction in the tails assume for now that the distribution of temperatures is driven by the family of symmetric Student-t distributions with zero mean. For these distributions, reaction in the left tail implies an increase in $\lambda^L$ degrees of freedom for each degree Celsius the average temperature increases over a given year. This increase in degrees of freedom entails a thinner left tail and, hence, a decrease in the likelihood of extreme negative temperatures. Similarly, reaction in the right tail entails a decrease in $\lambda^R$ degrees of freedom for an increase of one degree Celsius. This decrease in degrees of freedom entails a thicker right tail and, hence, an

increase in the likelihood of extreme positive temperatures.[4].

## 4. Tail parameter estimation

The tail parameters are not directly observed unless the data generating process of temperatures is known. In our application below, these parameters are estimated using cross-sectional information on monthly temperatures from climate stations around the globe. This process yields a time series of estimates, denoted as $(\widehat{\xi}_1, \ldots, \widehat{\xi}_T)$, which is then used for testing the presence of trends and reaction effects in both tails.

### 4.1. *Review of popular estimators*

Estimation of the tail parameter is indeed challenging, primarily because it depends on a nuisance parameter that determines the number of observations defining the tail of the distribution. Despite this difficulty, or perhaps because of it, the EVT literature has developed over one hundred estimators of the tail parameter (see Fedotenkov, 2018). Early and widely used estimators, such as the Hill (1975) and Pickands (1975) estimators, are derived as conditional maximum likelihood estimators of Pareto and Generalized Pareto distributions, respectively. These estimators are employed to model the tail decay of a broad class of parent distributions.

For illustrative purposes, we will focus on the right tail. The version of the Hill estimator for the tail parameter $\xi^R$ is

$$\widehat{\xi}_H^R = \left[ \frac{1}{k} \sum_{i=1}^{k} log\left(x_{i:n}/x_{k+1:n}\right) \right]^{-1}, \tag{6}$$

where $x_{1:n} > \ldots > x_{k+1:n}$ denote the first $k+1$ order statistics of the random sample $(x_1, \ldots, x_n)$. The order statistic $x_{k+1:n}$ can be interpreted as the threshold value that determines the Pareto behavior in the tail of the parent distribution. Hill's estimator is consistent for $\xi > 0$ under suitable choices of $x_{k+1:n}$ characterized by the conditions $k, n \to \infty$ with $k/n \to 0$. Pickands' (1975) estimator of the tail parameter $\xi^R$ is defined as

$$\widehat{\xi}_P^R(i) = \frac{log(2)}{log\left((x_{i:n} - x_{2i:n})/(x_{2i:n} - x_{4i:n})\right)}, \quad \text{for } i = 1, \ldots, k. \tag{7}$$

In contrast to the Hill estimator, Pickands' estimator is consistent for any $\xi \in \mathbb{R}$ and intermediate sequence $k \to \infty$ with $k/n \to 0$. Another important advantage of the latter estimator compared to most estimators of the tail parameter is its invariance under shift and scale transformations of the observations. Other estimators of the tail parameter also invariant to location shifts are developed in Fraga Alves (2001), Aban and Meerschaert (2001), and Ling et al (2007a, 2007b, 2012), among a few others. A refined version of the estimator (7) is provided by Drees (1995). This author

[4]The implications of this phenomena on the probability of tail events depend on the magnitude of the degrees of freedom parameter. For example, for a Student-t distribution with mean equal to 10, standard deviation equal to 10, and 15 degrees of freedom (similar values are observed for Europe and Asia since 2000 corresponding to the mean temperature and tail parameter, respectively) the probability of exceeding 30 degrees Celsius is 0.032.

introduces an estimator of $\xi^R$ that is constructed as a weighted mixture of Pickands' estimators computed over different values of $i = 1, \ldots, k$. The weights are generated by a probability measure which satisfies certain integrability condition. Other well known consistent estimators of the tail parameter based on the above estimators are the moment estimator of Dekkers, Einmahl and de Haan (1989), the method of moments ratio estimator proposed in Danielsson, Jansen and De Vries (1996), and more recently, the generalized least square estimator of Aban and Meerschaert (2004) and the least squares estimator of Tripathi, Kumar and Petropoulos (2014).

An alternative approach to estimate the tail parameter is to plot the statistic of interest against a number of the sample upper-order statistics and then infer an appropriate value for the tail parameter from the properties of the resulting graph (Kratz and Resnick, 1996; Beirlant, Vynckler and Teugels, 1996). Inspired by this approach, regression-based estimation methods have attracted considerable attention among empirical researchers. One such alternative is the OLS-based log-log rank-size regression (Rosen and Resnick, 1980 and Gabaix, 1999) that is given by the OLS estimator from the regression

$$log(i - \gamma) = \alpha_0 - \xi^R log x_{i:n} + \varepsilon_i, \text{ with } i = 1, \ldots, k, \tag{8}$$

with $\gamma = 0$ and $\varepsilon_i$ an error term. The statistical properties of the Ordinary Least Squares (OLS) estimators of equation (8) have been extensively analyzed in Gabaix and Ioannides (2004) and Gabaix and Ibragimov (2012). The latter authors also propose an optimal version of these estimators by setting $\gamma = 1/2$.

A shortcoming common across these methods is their questionable performance in small and moderate samples. Huisman et al (2001) correct for the small-sample biases in these methods by constructing a weighted average of a sequence of tail parameter estimators obtained from different thresholds $x_{k+1:n}$, for $k = 10, \ldots, 100$. Another major drawback common across estimators of the tail parameter is their sensitivity to location transformations of the data, which is explored in more detail in the simulation exercise below[5].

### 4.2. *Simulation exercise*

The aforementioned battery of estimators for the tail parameter are statistically consistent, meaning they converge in probability to the true parameter as the sample size increases. However, there are notable finite-sample effects that arise even in very large samples due to the slow convergence rate (typically $\sqrt{k}$) of most estimators. These effects may be exacerbated by large values of the location parameters. To illustrate these effects, we investigate the finite-sample differences between versions of the Hill and regression-based estimators obtained from raw and demeaned data.[6]

More specifically, the simulation experiment aims to compare the finite-sample performance of the Hill estimator and Gabaix and Ibragimov's regression-based estimator introduced in equation (8). Four estimators of the tail parameter on the right tail are

[5] An exception to this sensitivity is the recent regression-based estimator developed by Nicolau and Rodrigues (2019). These authors provide a significant improvement over existing estimators by reducing bias, demonstrating resilience to the choice of tail length, and accommodating time dependence in the data.

[6] Whereas there are studies in the statistical literature on extremes gauging the finite-sample effects of location shifts in estimators of the tail parameter, these studies usually focus on distributions modeling behavior in the extremes, such as the GDP, Pareto, or Burr distributions, see, for example, Ling et al (2012). In the current setting, we are interested in assessing the finite-sample effects of applying these estimators to distributions used for modeling the entire dataset and not only conditional on the extremes.

considered: (i) Hill estimator computed from the order statistics of the raw data. (ii) Hill estimator from the order statistics of the sequence of demeaned data. (iii) Ordinary Least Squares (OLS) estimator of the regression equation (8) from the raw order statistics. (iv) OLS estimator of the regression equation (8) from the demeaned sequence of order statistics. Interestingly, the version of the Hill estimator obtained from demeaned data can be interpreted as a particular case of Fraga Alves (2001) location-invariant estimator of the tail parameter. However, in contrast to this author, we use the sample mean instead of an intermediate order statistic to correct for the presence of location effects. By doing so, we avoid the choice of an additional tuning parameter in the construction of the location-invariant estimator.

The Monte Carlo experiment follows these steps. First, the data generating process (DGP) is based on the family of symmetric Student-t distributions with degrees of freedom $\theta = 2, 5, 10$. In this family, the tail parameter $\xi$ is equal to the degrees of freedom of the distribution. Second, different choices of the location parameters $\mu = 1, 10$ are incorporated into the DGP. These processes are simulated for sample sizes $n = 1000$ and $10,000$ to capture differences, in large samples, between versions of both estimators computed from raw and demeaned data. Third, both estimators require tuning of the nuisance parameter $k$. A range of values for $k$ in the interval $[10, 100]$ is considered, following the related literature on tail parameter estimation. Finally, this procedure is repeated for $M = 1,000$ independent draws of $n$ observations to compute the root mean square error associated to each estimator as

$$RMSE(\xi) = \sqrt{\sum_{m=1}^{M} (\widehat{\xi}_m - \xi)^2 / M}.$$

This comprehensive simulation setup allows for a thorough assessment of the empirical performance of the estimators under various conditions, providing valuable insights into their relative strengths and weaknesses. Figure 1 reports the RMSE of the estimators for $\mu = 10^7$. Left panels report the RMSE for $n = 1,000$ and right panels for $n = 10,000$. The dotted lines correspond to the estimators obtained from demeaned data and the solid lines to the estimators obtained from raw data. The thick lines denote the Hill estimators and the thin lines the regression-based estimators.

The comparison of results across figures reveals several key findings: (1) Estimators obtained from demeaned data exhibit significantly better performance than estimators obtained from raw data for heavy-tailed distributions ($\xi = 2, 5, 10$) and large location parameters ($\mu = 10$); (2) Hill-type estimators generally outperform regression-based methods; (3) Regardless of the type of estimator (using raw or demeaned data), the RMSE increases as a function of $\xi$. These findings across sample sizes; (4) The RMSE slightly decreases with increasing sample size, however, this effect is limited due to the fixed number of order statistics used to construct the estimators, ranging from $[10, 100]$ for both sample sizes. Similar results are obtained for the analysis of the left tail and negative values of the location parameter.

[7] Unreported results available from the authors upon request illustrate the RMSE for $\mu = 1$.

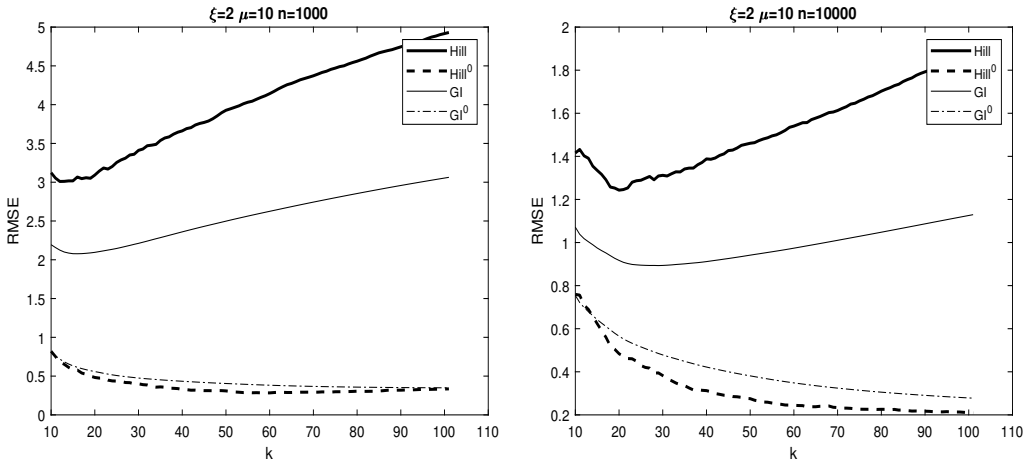


(a) $\xi = 2$, $n = 1,000$




(b) $\xi = 2$, $n = 10,000$

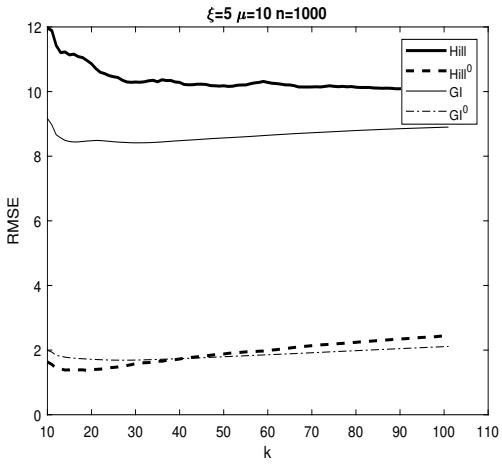


(c) $\xi = 5$, $n = 1,000$

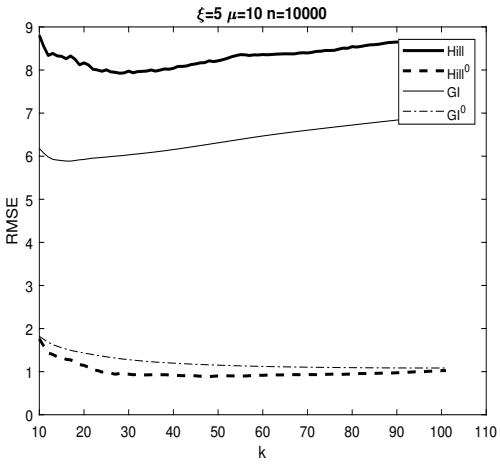


(d) $\xi = 5$, $n = 10,000$

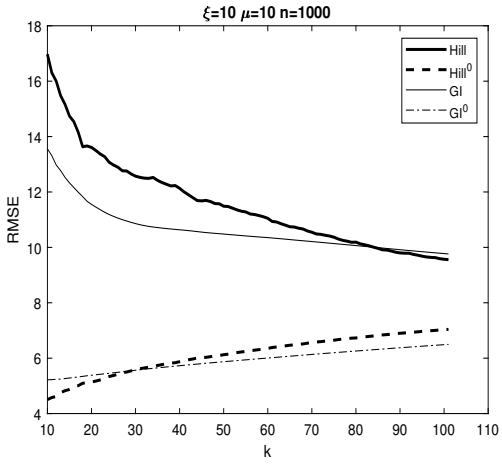


(e) $\xi = 10$, $n = 1,000$

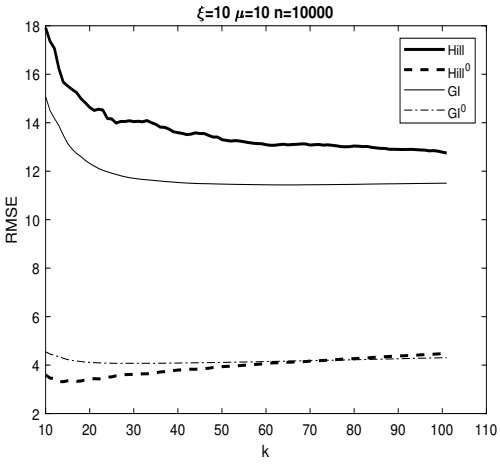


(f) $\xi = 10$, $n = 10,000$

**Figure 1.** Root mean square error for Hill estimator in (6) and regression-based estimator in (8); $k$ characterizes the threshold sequence $x_{k:n}$ and ranges in the interval $[10, 100]$. The data generating process is a Student-t distribution with $\xi$ degrees of freedom and location parameter $\mu = 10$.

## 5. Geographical heterogeneity in extreme warming

GG2020 and GG2025 document the existence of heterogeneity in the evolution of temperatures over time and across regions. This heterogeneity is often interpreted as evidence of positive trends in distributional characteristics such as the mean, median, and quantile processes, accompanied by a negative trend in dispersion measures. The objective of this section is to complement and expand upon these studies by analyzing the dynamics of extreme temperatures over time. To achieve this, we apply the trend tests introduced in Definitions 3 and 4 for the tail parameter $\xi$. These tests are applied to a panel of monthly temperatures for different regions of the world.

### 5.1. *Data*

The data used in this study originate from the Climatic Research Unit (CRU, https://crudata.uea.ac.uk/cru/data/temperature/) at the University of East Anglia, which provides monthly and yearly data of land temperatures in both hemispheres from 1850 to the present[8]. The proposed methodology to construct the database is described, among others, in Jones et al. (2012), Kennedy et al. (2019), and Osborn et al. (2021). For terrestrial regions worldwide, CRUTEM5.0 compiles time series of monthly mean temperatures based on data from more than 10,000 weather stations. These monthly mean temperatures are derived from daily observations, specifically as the average of the daily maximum and minimum temperatures. Let station $i$, in month $m$, and year $t$. We restrict our analysis to those station-month cross-section units that are present throughout the entire sample period, $t = 1, \ldots, T$. For each year $t$, we compute statistical summaries (e.g., mean, interquartile range, quantiles) based on all such station-month units available for that year. It is worth noting that the vast majority of stations included in the sample are consistently available across all months and years, with only a negligible number of exceptions. For instance, the annual mean temperature can be expressed as $C_t = \sum_{i=1}^{n} \sum_{m=1}^{12} \widetilde{X}_{i,m,t}$ where $\widetilde{X}_{i,m,t}$ represents the selected station's temperature in the month $m$ and year $t$.

For our study, we focus on the period from 1960 to 2022, which is a critical time-frame for climatological studies due to the increasing manifestation of climate change phenomena. There are several reasons for this choice of evaluation period. First, data availability: in regions with lower data density, starting the analysis in 1850 or 1880 would result in a sample with too few observations. While the number of available stations was limited in the 1850s, it increased to over 2,000 by 1900 and exceeded 5,000 for most of the 1951–2010 period (see Figure 8 in Osborn et al., 2021). Notably, the CRU database shows a significant expansion in station coverage across all global regions beginning in the 1960s. Second, there is empirical evidence of a structural break in the global temperature trend around this period, marked by a substantial increase in the slope (see, for example, Estrada and Perron, 2017 and Beaulieu et al. 2024). To ensure the stability of the characteristics over the entire sample period we select only those month-station units with data for all years within the sample period. Additionally, we remove stations presenting issues of inhomogeneities, as documented by Jones et al.

[8]The CRU dataset includes HadCRUT5, which offers gridded temperature anomalies across the world, as well as averages for the hemispheres and the globe. CRUTEM5 and HadSST4 represent the land and ocean components of this comprehensive dataset, respectively. HadCRUT5, in particular, has become one of the most widely used datasets to illustrate global warming trends, often depicted in the "hockey stick" graph, frequently referenced by academics and institutions such as the Intergovernmental Panel on Climate Change (IPCC).

(2012)[9]. After applying these selection criteria to the 1960-2022 sample period, we are left with a dataset comprising n=11,113 month-station units, originating from 1,150 stations out of a total of 10,575.

In addition to analyzing global trends, we adopt regional perspectives to provide more informative predictions at the regional level. For this purpose, we divide the globe into eight geographical areas: the Arctic Polar Circle, Europe, North America, South America, Asia, Africa, Australia, and Antarctica. Using the selection strategy described earlier, we obtain a total of 11,113 month-station observations for the entire globe. Among these observations, 472 are from the Arctic region, 3,227 from Europe, 2,413 from North America, 279 from South America, 4,655 from Asia, 261 from Africa, 457 from Australia, and 67 from Antarctica. To assign stations to their respective regions, we use a geographical approach based on latitude and longitude coordinates. Specifically, each station is assigned to a region based on the latitude and longitude rectangle that encompasses the continent it belongs to. This approach prioritizes the latitude variable over other classifications based solely on political boundaries.

Figure 2 illustrates the distribution of selected stations according to the unit month-station criterion for the entire globe during the period 1960-2022 and Figure 3 displays nonparametric kernel density estimates of the realized distribution of annual temperatures for each of the eight regions. These density functions are estimated from cross-sectional observations recorded at various weather stations within each region for a given year. The plots reveal distinct patterns across regions. The distributions of temperatures for Asia, North America, South America, and the Arctic region exhibit left skewness. The nonparametric kernel density functions for Europe and Australia are symmetric. The density function of temperatures for Africa is right-skewed with a mode around $15^o$ celsius and the right tail reaches values near $40^o$ celsius. The kernel density function for The Antarctic is bimodal and reflects the strong heterogeneity in temperatures across weather stations. The Western region is colder than the Eastern region.

### 5.2. *Analysis of trends in extreme temperatures*

This section investigates the tail behavior of the realized distribution of annual temperatures. To do this, we take advantage of the results obtained in the simulation exercise and use different versions of the Hill estimator applied to sequences of temperatures that are cross-sectionally demeaned using data from each of the eight regions and over each year of the evaluation period. This is so because there is clear evidence from the kernel density estimates in Figure 3 that the distributions of temperatures exhibit heavy tails and have a positive location parameter.

Table 1 presents a comprehensive set of summary statistics for the time series of estimates of the tail parameter, $\xi$, derived from the distribution of temperatures. To ensure the robustness of our findings we compute estimates of the tail parameter using various location-invariant versions of the Hill estimator. More specifically,

- Method 1 reports the Hill estimator.

[9]The decision to work with raw station data is intended to ensure stable behavior across the entire sample period; thus, our selection criterion is based on the consistent presence of stations throughout the study period. These stations are not necessarily located in large cities and are geographically well distributed. While it is true that station density is higher in more populated areas—such as the United States, southern Canada, Europe, and Japan—coverage is sparser in regions such as the interior of South America and Africa, as well as Antarctica. Nevertheless, this does not compromise our analysis, whose primary objective is to estimate temperature trends.

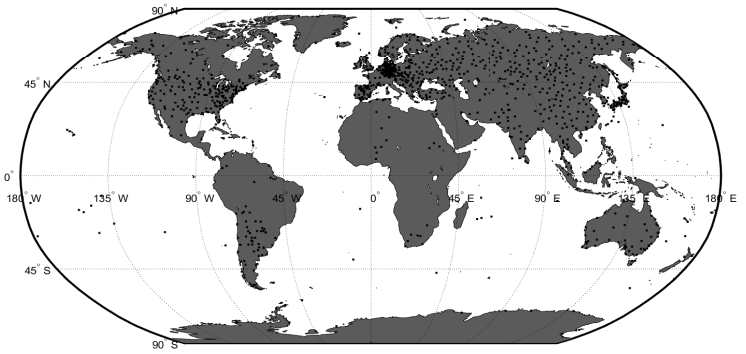


**Figure 2.** Location of weather stations 1960-2022.

- Method 2 reports the generalized least square estimator proposed by Aban and Meerschaert (2004).
- Method 3 reports the least squares estimator introduced in Tripathi, Kumar and Petropoulos (2014).

Furthermore, to account for the dependence of the methods on the specific choice of the threshold sequence $k$, see (6), we report the Huisman et al. (2001) correction of the above three estimators.

For each region and year within the evaluation period we obtain estimates of the tail parameter resulting in a sample of 63 time series estimates for each region. The results presented in Table 1 demonstrate the similarity of the tail parameter estimates across estimation methods. The sample standard deviations obtained from the time series are small and suggest little time variation of the tail parameter estimates. The minimum and maximum statistics also offer further insights into the dispersion of the parameter estimates of $\xi$ over time.

It is crucial to acknowledge that the dynamics of the tail parameter alone do not provide a comprehensive characterization of extreme temperatures. To gain a better understanding, this analysis must be supplemented with the analysis of other distributional characteristics such as the mean, standard deviation, and various centrality measures. This can be done by considering the joint dynamics between mean temperatures and tail behavior, as encapsulated by the concept of warming reaction in Definition 4. Therefore, the subsequent discussion is built upon the results showcased in Tables 2 to 4,[10] along with the visual representations provided in Figures 4 to 6, which illustrate the evolution of the mean, standard deviation, and tail parameters throughout the evaluation period (1960-2022).

Our findings regarding the dynamics of the tail parameter exhibit parallels with the examination of trends in maximum and minimum temperatures. Both analyses offer

[10]Reported p-values correspond to t-tests obtained from HAC robust standard errors using a Bartlett kernel with a data-driven bandwidth, see Newey and West (1987) and Andrews (1991).

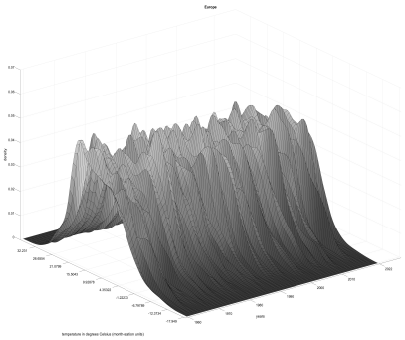

(a) Europe

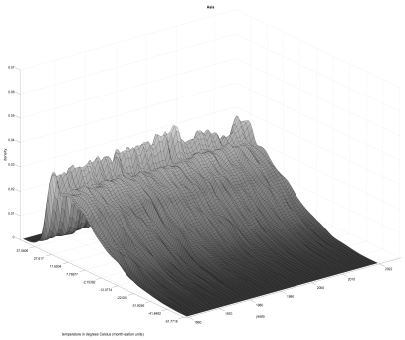

(b) Asia

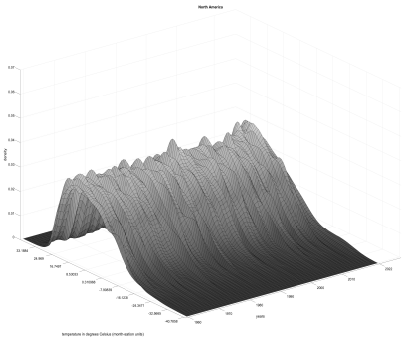

(c) North America

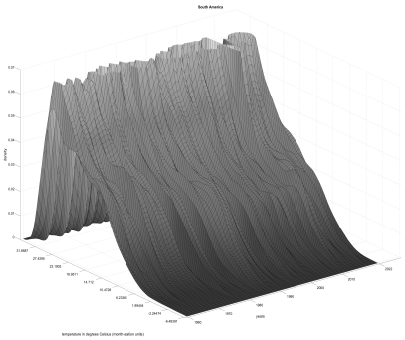

(d) South America

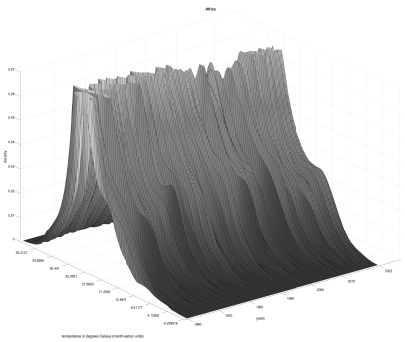

(e) Africa

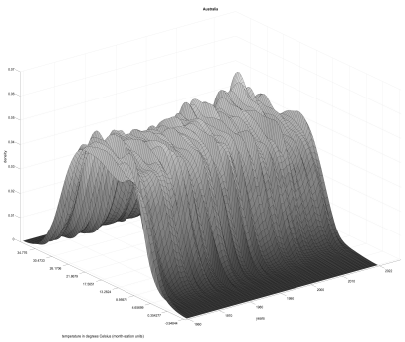

(f) Australia

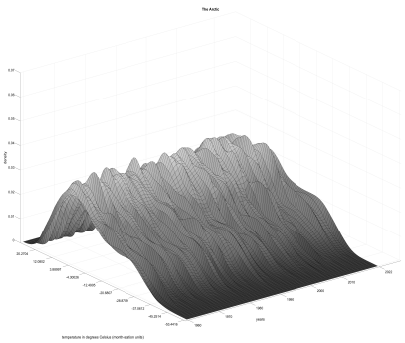

(g) Arctic Polar Circle

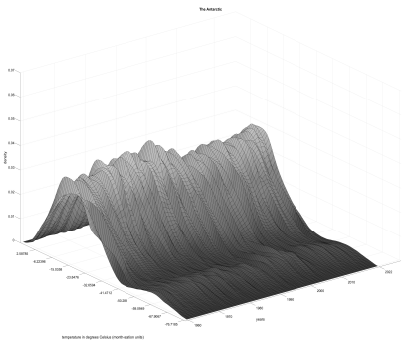

(h) Antarctica

**Figure 3.** Kernel density function estimates for annual temperatures (1960-2022).

**Table 1.** Summary statistics of the sequence of tail parameter estimators using Huisman et al (2001) type estimator.

| | Sample mean | | | | | | Standard deviation | | | | | | Minimum | | | | | | Maximum | | | | | |
|---|---|---|---|---|---|---|---|---|---|---|---|---|---|---|---|---|---|---|---|---|---|---|---|---|
| | Left | | | Right | | | Left | | | Right | | | Left | | | Right | | | Left | | | Right | | |
| Region/Method | 1 | 2 | 3 | 1 | 2 | 3 | 1 | 2 | 3 | 1 | 2 | 3 | 1 | 2 | 3 | 1 | 2 | 3 | 1 | 2 | 3 | 1 | 2 | 3 |
| Globe | 8.1 | 7.8 | 7.0 | 18.0 | 17.1 | 15.5 | 1.3 | 1.2 | 1.2 | 2.2 | 2.1 | 2.0 | 6.3 | 6.0 | 5.4 | 14.2 | 13.5 | 12.0 | 11.7 | 11.3 | 10.3 | 24.2 | 23.1 | 20.9 |
| Europe | 11.3 | 10.8 | 9.8 | 17.1 | 16.4 | 14.9 | 3.5 | 3.4 | 3.1 | 2.5 | 2.4 | 2.2 | 5.1 | 4.8 | 4.3 | 9.8 | 9.3 | 8.4 | 21.7 | 20.8 | 18.8 | 23.5 | 22.5 | 20.5 |
| Asia | 16.8 | 16.1 | 14.6 | 18.2 | 17.3 | 15.7 | 3.1 | 3.0 | 2.7 | 2.7 | 2.6 | 2.4 | 10.9 | 10.4 | 9.4 | 13.4 | 12.8 | 11.4 | 24.8 | 23.7 | 21.5 | 25.3 | 24.2 | 21.9 |
| North America | 12.2 | 11.6 | 10.6 | 19.8 | 18.9 | 17.2 | 1.7 | 1.6 | 1.5 | 3.9 | 3.8 | 3.5 | 9.1 | 8.7 | 7.9 | 13.5 | 12.9 | 11.6 | 16.7 | 16.0 | 14.6 | 34.7 | 33.3 | 30.6 |
| South America | 6.6 | 6.3 | 5.7 | 14.6 | 13.9 | 12.6 | 0.6 | 0.6 | 0.6 | 2.9 | 2.8 | 2.5 | 5.3 | 5.1 | 4.6 | 9.4 | 8.9 | 8.1 | 8.5 | 8.1 | 7.4 | 22.3 | 21.3 | 19.3 |
| Africa | 5.3 | 4.9 | 4.2 | 5.2 | 4.9 | 4.2 | 0.7 | 0.6 | 0.6 | 0.8 | 0.7 | 0.7 | 4.1 | 3.8 | 3.3 | 3.9 | 3.6 | 3.1 | 7.5 | 7.0 | 6.1 | 9.3 | 8.7 | 7.6 |
| Australia | 8.6 | 8.3 | 7.5 | 9.1 | 8.7 | 7.9 | 0.8 | 0.8 | 0.7 | 1.1 | 1.1 | 1.0 | 7.0 | 6.7 | 6.1 | 6.7 | 6.4 | 5.8 | 11.5 | 10.9 | 9.8 | 12.8 | 12.2 | 11.1 |
| Arctic Circle | 8.3 | 7.9 | 7.2 | 14.1 | 13.5 | 12.2 | 1.3 | 1.2 | 1.1 | 2.6 | 2.4 | 2.2 | 5.8 | 5.5 | 5.0 | 9.3 | 8.9 | 8.1 | 11.5 | 11.0 | 10.1 | 22.3 | 21.3 | 19.2 |
| Antarctica | 1.7 | 1.5 | 1.0 | 9.6 | 8.4 | 6.0 | 0.6 | 0.5 | 0.4 | 3.3 | 3.0 | 2.5 | 0.5 | 0.4 | 0.2 | 4.2 | 3.4 | 1.8 | 3.2 | 2.9 | 2.2 | 22.4 | 20.1 | 15.3 |

Note: These summary statistics are computed from a time series of tail parameter estimates. Method 1 is the small-sample correction of the Hill estimator; Method 2 is the correction of the generalized least square estimator proposed in Aban and Meerschaert (2004), and Method 3 is the correction of the least squares estimator obtained in Tripathi (2014). The time series of estimates of $\xi$ are obtained from cross-sections of monthly temperatures recorded for each region and year over the period 1960 to 2022.

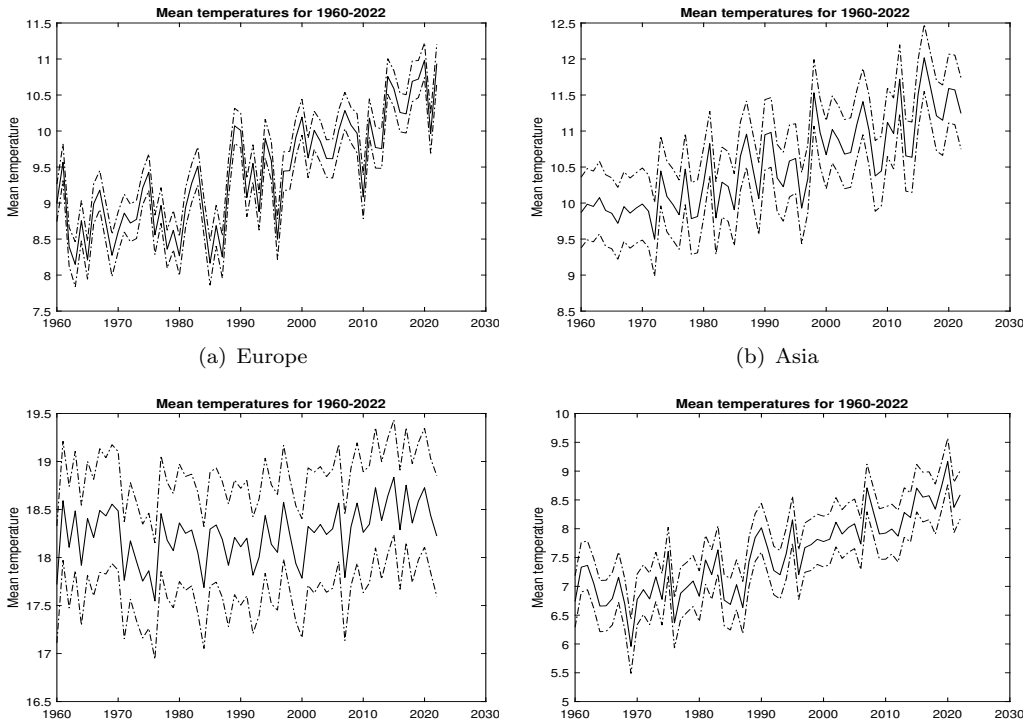


(a) Europe (b) Asia

(c) North America (d) South America

**Figure 4.** Dynamics of cross-sectional mean temperatures for a subset of representative regions over the period 1960-2022. Dotted lines are 95% confidence intervals.

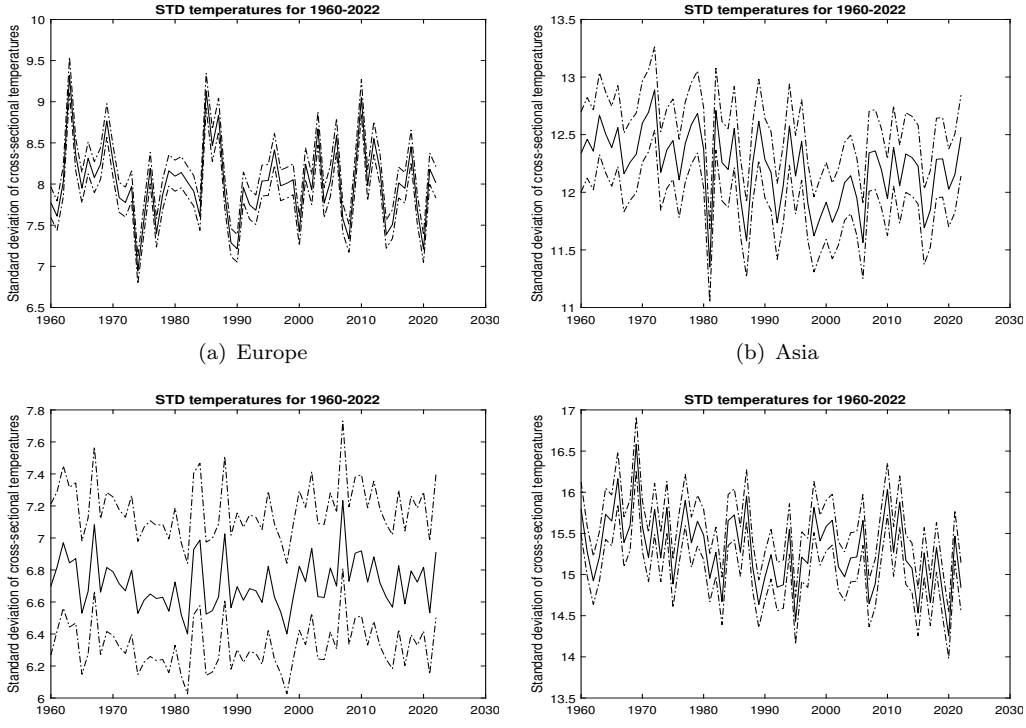


(a) Europe (b) Asia

(c) North America (d) South America

**Figure 5.** Dynamics of cross-sectional standard deviations of temperatures for a subset of representative regions over the period 1960-2022. Dotted lines are 95% confidence intervals.

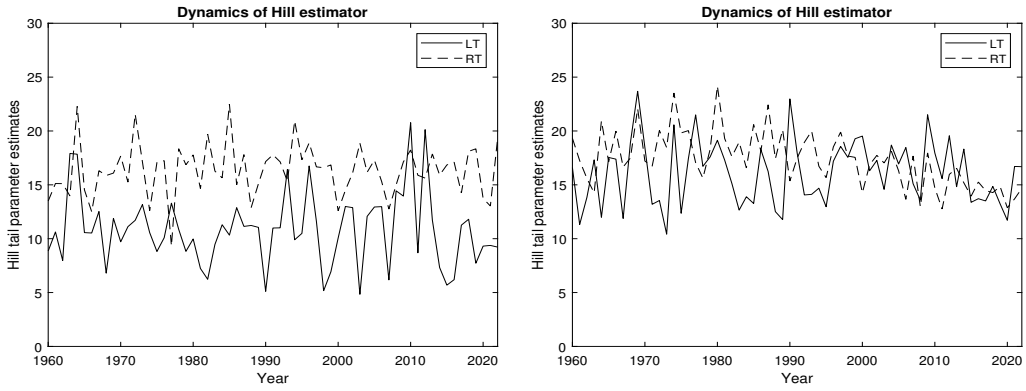


(a) Europe




(b) Asia

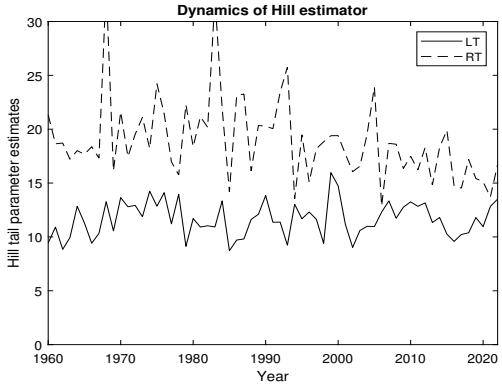


(c) North America

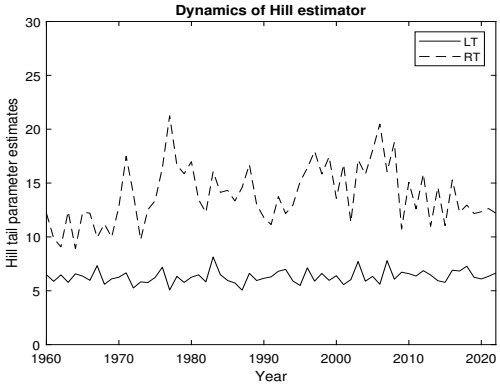


(d) South America

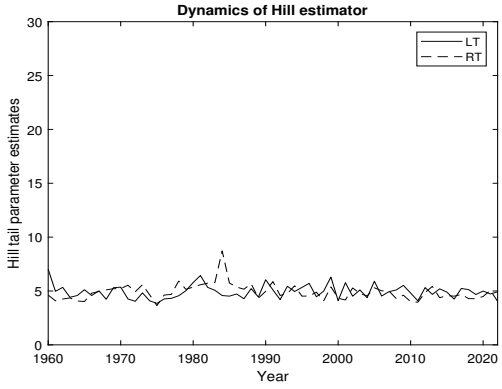


(e) Africa

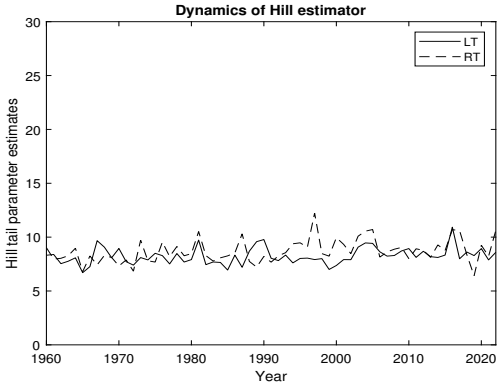


(f) Australia

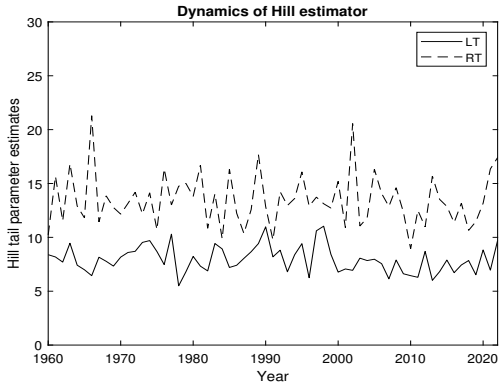


(g) Arctic Polar Circle

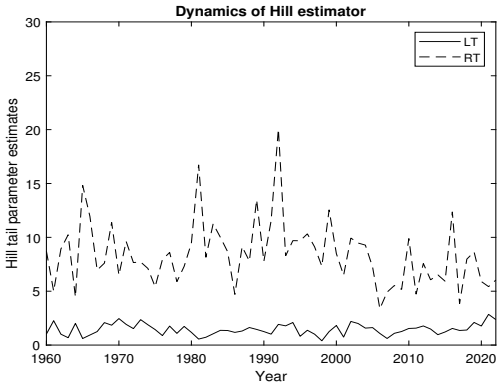


(h) Antarctica

**Figure 6.** Dynamics of Huisman small-sample correction of Hill estimator for the realized distribution of annual temperatures (1960-2022).

evidence of extreme warming. However, a key distinction lies in the representativeness of the results. The analysis of maximum and minimum temperatures typically relies on a single annual observation. This observation is recorded at a specific weather station over time and, hence, may lack representativeness with regards to the study of extreme warming for a wider region. In contrast, the estimation of the tail parameter involves aggregating data from the $k$ largest or smallest observations across all stations within a region for 12 months. This method provides a more comprehensive view of the overall dynamics of extreme temperatures for a specific region. Despite this advantage, interpreting trends based on tail parameter estimates can be more complex compared to interpretations based on extreme statistics like maxima and minima. Nonetheless, by employing the dynamics of tail parameters, we gain a deeper understanding of the evolution of extreme temperatures over time, thereby enhancing our ability to model and address climate change impacts effectively.

**The Globe**

This region pools together all available observations. Table 1 highlights notable heterogeneity across tails. Specifically, the left tail demonstrates a polynomial decay, with $\xi$ estimates hovering around 7.5, while the right tail exhibits a more rapid decay, indicated by estimates around 17. In Table 2, the trend test results are noteworthy. While the left tail shows no statistically significant trend, the right tail exhibits a negative trend for $\xi_t^R$ that is statistically significant at 5%. The implication of this result is that the tail parameter diminishes over time, resulting in a thicker tail and, consequently, an increased likelihood of positive extreme events. This type of tail behavior aligns with the classification of extreme warming WE2 given in Definition 2.

Quantitatively, using expression (1), it follows that $P\{X_t > x\} = 1 - F(x) = x^{-\xi_t^R}\mathcal{L}(x)$, for $x > 1$, such that $\frac{P\{X_{t+1}>x\}}{P\{X_t>x\}} = x^{-(\xi_{t+1}^R - \xi_t^R)} > 1$ implying that $P\{X_{t+1} > x\} > P\{X_t > x\}$ if $\xi_{t+1}^R - \xi_t^R < 0$. Table 2 reports a value of $\beta$ of $-0.038$ for the Globe using the estimation method 1. Furthermore, using the linear time trend formulation of the tail parameter in (3), it follows that $E[\xi_{t+1}^R - \xi_t^R] = \beta$ and, using the above argument, the ratio of tail probabilities between Year $t$ and $t+1$ can be approximated by $x^{0.038}$. Thus, using expression (2) in Remark 2, the ratio of tail probabilities for the random variable of annual temperature $Y$, with mean $\mu$ and standard deviation $\sigma$, is

$$\frac{P\{Y_{t+1} > y\}}{P\{Y_t > y\}} = \left(\frac{y-\mu}{\sigma}\right)^{0.038},$$

for $y > \mu$. For example, for $y = 30$ degrees Celsius, with $\mu = 10$ and $\sigma = 10$ (average values of the mean and standard deviation of the time series of temperatures for the Globe), we obtain $\frac{P\{Y_{t+1}>y\}}{P\{Y_t>y\}} = 2^{0.038}$, such that $P\{Y_{t+1} > y\} = 1.0267P\{Y_t > y\}$. This result estimates an increase of 2.6% in the probability of reaching more than 30 degrees Celsius between consecutive years in the evaluation period for the Globe.

Table 3 presents the outcomes of the trend tests for centrality and dispersion measures. For the Globe, all centrality measures exhibit a robust positive trend, including the mean, alongside a decrease in dispersion. Moreover, the low and top quantiles also demonstrate a trend, indicating a global rightward shift in the temperature distribution. These findings are further substantiated by the analysis of comovements between the mean process and tail behavior in Table 4.[11] The negative slope parameter es-

[11] Unreported results, testing for unit roots using the Augmented Dickey-Fuller test, ascertain the stationarity of the residuals in such regressions, confirming the stability of the findings in Table 4. Additionally, tests for a

timates obtained from regression (5) suggest a reaction effect in the right tail. This implies that extreme temperatures in the right of the distribution are warming faster over time than implied by the positive shift of the mean process documented in Table 3. In contrast, for the left tail, the negative estimates obtained from regression (4) do not indicate a reaction effect. Instead, the estimates of the slope coefficient $\lambda^L$ suggest that negative extreme temperatures experience a slower shift to the right than the corresponding low quantiles, which undergo faster right shifts. These empirical findings lead to an increase in dispersion in the left tail of the distribution of temperatures.

Indeed, Table 3 highlights the presence of a positive trend for maximum temperatures and a negative trend, albeit statistically insignificant, for minimum temperatures. This disparity underscores the complexity of temperature dynamics, revealing distinct trends across various temperature metrics. Such findings underscore the nuanced nature of climate change impacts, where different temperature components may exhibit differential responses over time.

**The Northern hemisphere**

The observations regarding North America and Asia indicate pronounced trends in extreme warming, consistent with the global analysis. Both regions exhibit significant decreases in the tail parameter estimates in Table 2 over the study period, indicative of a fatter tail and an increased likelihood of extreme positive temperatures. This trend is particularly notable given the substantial magnitude of the slope coefficients, which are roughly twice as large as those observed for the Globe. The quantitative increase in the probability of extreme events in the right tail for these regions can be computed using the above expressions but using the estimates of $\beta$ obtained for North America and Asia reported in Table 2. The visual representation provided in Figure 6 also corroborates these findings, illustrating the steady decline in the tail parameter estimates over the past six decades. Additionally, nonlinearities observed in the Asian region between 1970 and 1990 suggest potential variations in the warming pattern during this period, warranting further investigation into regional climate dynamics.

The consistency in dynamics observed across North America and Asia mirrors the trends seen globally, with notable shifts in both centrality and dispersion measures indicating an overall warming trend and decreased variability in temperature distributions. The reaction analysis between the mean process and the right tail parameter reported in the right panel of Table 4 reinforces the evidence of extreme warming exceeding that suggested by changes in the mean process. The parameter estimates are negative and the null hypothesis $H_{0RR}$ is rejected at 1% significance level for both regions. However, in line with the results found for The Globe, there is no empirical evidence of reaction effects for the left tail. The negative slopes reported in the left panel of Table 4 for Asia and North America suggest that the extreme negative temperatures shift to the right at a slower pace than temperatures in the lower, but not extreme, quantiles. These findings underscore the complex interplay between mean temperatures and extreme events, highlighting the need for comprehensive approaches to understand regional climate dynamics.

The analysis of Europe presents a distinct pattern compared to North America and Asia. The empirical estimates indicate a thicker average tail, but the trend tests do not reveal statistically significant trends in either tail. This absence of extreme warming trends is consistent with a scenario where extreme events remain relatively

time trend in the residuals refute the presence of such trends, bolstering the evidence for the pure stationarity of the residuals in all cases. Consequently, the results in Table 4 capture the correlation between the tail parameters and mean temperatures for each region over time, devoid of spurious relationships.

stable over time (WE0 type). In contrast, mean temperatures exhibit a positive trend, while dispersion measures show no significant changes over time, indicating a uniform shift in the realized distribution of annual temperatures. Similar findings are obtained by Ballester et al. (2010). Additionally, the lack of statistical evidence for a reaction between tail and location parameters in both tails suggests that extreme temperatures in Europe do not shift at a faster pace than what is implied by changes in the mean process alone.

The analysis of the Arctic Polar Circle reveals a statistically significant negative trend in the left tail at 10% significance level. This result indicates the presence of a heavier left tail in the realized distribution of annual temperatures over time. This trend is accompanied by a positive and statistically significant trend in the mean and low quantiles as documented in Table 3. This combination of effects is interpreted as a relative shift in the low quantiles of the distribution of temperatures compared to the extreme quantiles. In contrast, the evidence for extreme warming in the right tail is weak and not statistically significant.

**The Southern hemisphere**

The analysis of South America and Australia reveals a statistically significant positive slope for the regression coefficient of equation (3), indicating thinner left tails over time for both regions. For the left tail, the warming determined by a positive trend is of type WE1 and reflects an increase in the value of extreme temperatures becoming milder over time. More specifically, applying expression (1) to the left tail of the distribution, it follows that $P\{X_t \leq x\} \approx (-x)^{-\xi_t^L}$, for $x < 0$ sufficiently in the tail (i.e. $|x| > 1$). Furthermore, for $\beta > 0$, expression (3) implies that $E[\xi_{t+1}^L - \xi_t^L] = \beta > 0$, and then

$$\frac{P\{X_{t+1} \leq x\}}{P\{X_t \leq x\}} \approx (-x)^{-\beta} < 1.$$

If $Y$ denotes the realized location-scale distribution of annual temperatures, with mean $\mu$ and standard deviation $\sigma$, it follows that $\frac{P\{Y_{t+1} \leq y\}}{P\{Y_t \leq y\}} \approx \left(-\frac{y-\mu}{\sigma}\right)^{-0.006}$ for South America and $\frac{P\{Y_{t+1} \leq y\}}{P\{Y_t \leq y\}} \approx \left(-\frac{y-\mu}{\sigma}\right)^{-0.011}$ for Australia. For example, for $y = 0$ degrees Celsius, with $\mu = 9$ and $\sigma = 6$ (average values of the mean and standard deviation of the time series of temperatures for South America), we obtain $P\{Y_{t+1} \leq y\} \approx 1.5^{-0.006} P\{Y_t \leq y\}$. Similarly, for Australia, we obtain (unreported values) $\mu = 18$ and $\sigma = 6$ such that $P\{Y_{t+1} \leq y\} \approx 3^{-0.011} P\{Y_t \leq y\}$. These results suggest that the probability of reaching temperatures below zero decreases by 0.24% over two consecutive years for South America and by 1.2% for Australia.

These results provide strong statistical evidence of warming in the left tail of the distribution of temperatures for these regions from the Southern Hemisphere. This conclusion is further supported by the tail reaction analysis reported in Table 4. Both regions show a positive coefficient and robust p-values that reject the null hypothesis $H_{0RL} : \lambda^L \leq 0$ against the hypothesis $H_{ARL} : \lambda^L > 0$ at 5% significance level. Therefore, the positive shift in extreme temperatures in the left tail is beyond what would be implied by a location shift.

The results for Africa and the Antarctic region in Table 2 are less conclusive, showing no statistical evidence of extreme warming in the left tail. The sign of the trend parameter in regression (4) is positive but not statistically significant to reject the null hypothesis $H_{0TL}$. The analysis of tail warming reaction in Table 4 provides no evidence of reaction in the left tail for both Africa and Antarctica. In contrast, the sign of the

**Table 2.** Trending analysis for standardized temperatures under regression equation (3).

| | Left tail | | | Right tail | | |
|---|---|---|---|---|---|---|
| Region/Method | 1 | 2 | 3 | 1 | 2 | 3 |
| Globe | -0.012 | -0.011 | -0.010 | $-0.038^{**}$ | $-0.037^{**}$ | $-0.033^{**}$ |
| *c.i.* | [-0.029,0.006] | [-0.029,0.005] | [-0.028,0.004] | [-0.068,-0.008] | [-0.067,-0.010] | [-0.065,-0.012] |
| *p-value* | [0.189] | [0.207] | [0.247] | [0.011] | [0.012] | [0.014] |
| Europe | -0.010 | -0.010 | -0.009 | 0.007 | 0.007 | 0.005 |
| *c.i.* | [-0.062,0.043] | [-0.060,0.041] | [-0.056,0.036] | [-0.023,0.038] | [-0.022,0.037] | [-0.020,0.035] |
| *p-value* | [0.721] | [0.712] | [0.691] | [0.640] | [0.662] | [0.711] |
| Asia | 0.002 | 0.001 | 0.002 | $-0.080^{***}$ | $-0.077^{***}$ | $-0.070^{***}$ |
| *c.i.* | [-0.044,0.044] | [-0.042,0.042] | [-0.038,0.038] | [-0.111,-0.048] | [-0.110,-0.049] | [-0.107,-0.052] |
| *p-value* | [0.992] | [0.965] | [0.902] | [0.000] | [0.000] | [0.000] |
| North America | 0.008 | 0.008 | 0.007 | $-0.076^{***}$ | $-0.073^{***}$ | $-0.068^{***}$ |
| *c.i.* | [-0.018,0.035] | [-0.017,0.033] | [-0.014,0.031] | [-0.068,-0.008] | [-0.120,-0.032] | [-0.115,-0.036] |
| *p-value* | [0.532] | [0.527] | [0.515] | [0.001] | [0.001] | [0.001] |
| South America | $0.006^{**}$ | $0.006^{**}$ | $0.006^{**}$ | 0.034 | 0.033 | 0.031 |
| *c.i.* | [0.001,0.012] | [0.001,0.012] | [0.001,0.012] | [-0.023,0.092] | [-0.021,0.090] | [-0.017,0.085] |
| *p-value* | [0.032] | [0.032] | [0.032] | [0.239] | [0.238] | [0.236] |
| Africa | 0.000 | 0.001 | 0.001 | -0.007 | -0.006 | -0.005 |
| *c.i.* | [-0.009,0.010] | [-0.008,0.009] | [-0.007,0.008] | [-0.020,0.007] | [-0.019,0.006] | [-0.017,0.004] |
| *p-value* | [0.921] | [0.901] | [0.853] | [0.323] | [0.323] | [0.322] |
| Australia | $0.011^{**}$ | $0.011^{**}$ | $0.009^{**}$ | $0.021^{***}$ | $0.021^{***}$ | $0.019^{***}$ |
| *c.i.* | [0.001,0.022] | [0.001,0.021] | [0.002,0.020] | [0.007,0.036] | [0.007,0.035] | [0.009,0.034] |
| *p-value* | [0.030] | [0.033] | [0.040] | [0.004] | [0.004] | [0.004] |
| Arctic Circle | $-0.013^{*}$ | $-0.012^{*}$ | $-0.012^{*}$ | −0.007 | −0.006 | −0.005 |
| *c.i.* | [-0.027,0.002] | [-0.027,0.002] | [-0.026,0.000] | [-0.040,0.026] | [-0.038,0.024] | [-0.035,0.021] |
| *p-value* | [0.094] | [0.090] | [0.082] | [0.677] | [0.686] | [0.705] |
| Antarctica | 0.003 | 0.003 | 0.002 | $-0.039^{*}$ | $-0.036^{*}$ | $-0.028^{*}$ |
| *c.i.* | [-0.007,0.014] | [-0.006,0.013] | [-0.004,0.011] | [-0.078,0.000] | [-0.075,-0.003] | [-0.068,-0.010] |
| | [0.522] | [0.528] | [0.542] | [0.050] | [0.051] | [0.056] |

Note: Confidence intervals at 95% significance levels and p-values (in square brackets) are obtained from HAC robust standard errors. $*$, $**$, $***$ denote statistical significance of the robust slope parameter estimate $\beta$ of the LS regression equation (3) at 10%, 5% and 1% significance levels, respectively. The response variable is the sequence of tail parameter estimates $\widehat{\xi}_t^L$ and $\widehat{\xi}_t^R$ obtained under different estimation methods. Method 1 is the small-sample correction of the Hill estimator; Method 2 is the correction of the generalized least square estimator proposed in Aban and Meerschaert (2004), and Method 3 is the correction of the least squares estimator obtained in Tripathi (2014). The time series of estimates of $\xi$ are obtained from cross-sections of monthly temperatures recorded for each region and year over the period 1960 to 2022.

trend parameter estimate for the right tail reported in Table 2 is negative for both regions but only statistically significant for Antarctica at 10%. This result provides weak evidence of warming type WE2 for this region. This result is reinforced by the analysis in Table 4 that reveals statistical evidence of warming reaction in the right tail for the Antarctic region at 5%. Extremes in the right tail of the realized distribution of temperatures shift faster to the right than high quantiles for Antarctica but not for Africa.

## 6. Conclusion

This study provides a comprehensive analysis of the dynamics of extreme temperatures, offering valuable insights into the heterogeneity of climate change effects across different regions and seasons. By focusing on the tail parameter and proposing a

**Table 3.** Trend tests (Globe areas,1960-2022)

| Characteristic | Globe | Arctic Circle | Europe | North-Am. | South-Am. | Asia | Africa | Australia | Antarctica |
|---|---|---|---|---|---|---|---|---|---|
| mean | 0.030 | 0.053 | 0.033 | 0.027 | 0.005 | 0.032 | 0.024 | 0.019 | 0.002 |
| | [0.000] | [0.000] | [0.000] | [0.000] | [0.029] | [0.000] | [0.000] | [0.000] | [0.455] |
| max | 0.020 | 0.021 | 0.037 | 0.047 | 0.005 | 0.020 | 0.047 | 0.021 | -0.005 |
| | [0.001] | [0.017] | [0.000] | [0.000] | [0.557] | [0.001] | [0.000] | [0.002] | [0.313] |
| min | -0.014 | 0.047 | 0.071 | 0.090 | 0.016 | 0.047 | 0.014 | 0.034 | -0.014 |
| | [0.192] | [0.000] | [0.000] | [0.000] | [0.000] | [0.000] | [0.105] | [0.000] | [0.192] |
| std | -0.007 | -0.014 | -0.002 | -0.007 | -0.000 | -0.009 | 0.006 | -0.000 | -0.000 |
| | [0.000] | [0.000] | [0.440] | [0.001] | [0.762] | [0.002] | [0.000] | [0.821] | [0.903] |
| iqr | -0.006 | -0.034 | -0.004 | -0.002 | -0.003 | -0.012 | 0.007 | 0.001 | 0.011 |
| | [0.048] | [0.000] | [0.310] | [0.681] | [0.261] | [0.000] | [0.006] | [0.812] | [0.306] |
| rank | 0.034 | -0.026 | -0.034 | -0.043 | -0.011 | -0.027 | 0.033 | -0.013 | 0.009 |
| | (0.000) | (0.095) | (0.041) | (0.005) | (0.248) | (0.041) | (0.000) | (0.100) | (0.456) |
| kur | 0.002 | 0.003 | -0.002 | -0.004 | -0.000 | 0.001 | -0.000 | -0.001 | 0.001 |
| | [0.161] | [0.000] | [0.124] | [0.004] | [0.320] | [0.037] | [0.641] | [0.114] | [0.452] |
| skw | 0.000 | -0.002 | 0.004 | 0.002 | -0.000 | -0.000 | -0.000 | -0.000 | -0.000 |
| | [0.550] | [0.000] | [0.000] | [0.000] | [0.589] | [0.485] | [0.398] | [0.298] | [0.686] |
| q05 | 0.046 | 0.058 | 0.048 | 0.043 | 0.005 | 0.048 | 0.013 | 0.015 | -0.000 |
| | [0.000] | [0.000] | [0.000] | [0.000] | [0.064] | [0.000] | [0.001] | [0.000] | [0.993] |
| q10 | 0.047 | 0.070 | 0.044 | 0.036 | 0.005 | 0.051 | 0.014 | 0.018 | 0.013 |
| | [0.000] | [0.000] | [0.000] | [0.000] | [0.038] | [0.000] | [0.000] | [0.000] | [0.096] |
| q90 | 0.023 | 0.028 | 0.042 | 0.0247 | 0.007 | 0.021 | 0.030 | 0.020 | 0.007 |
| | [0.000] | [0.000] | [0.000] | [0.000] | [0.025] | [0.000] | [0.000] | [0.000] | [0.031] |
| q95 | 0.021 | 0.028 | 0.042 | 0.025 | 0.005 | 0.019 | 0.034 | 0.018 | -0.001 |
| | [0.000] | [0.000] | [0.000] | [0.000] | [0.225] | [0.000] | [0.000] | [0.000] | [0.849] |

Note: Annual distributional characteristics of temperature from monthly CRU data (1960-2022). OLS estimates and HAC $t_{\beta=0}$ from regression: $C_t = \alpha + \beta t + u_t$, where $C_t$ is a vector of distributional characteristics (mean (*mean*), standard deviation (*std*), maximum (*max*), minimum (*min*), interquartile range (*iqr*), total range (*range*), kurtosis (*kur*), skewness (*skw*), and a sequence of quantiles) estimated from $N$ observations for each year.

**Table 4.** Tail warming reaction effects for annual temperatures using regressions (4) and (5).

| | Left tail | | | Right tail | | |
|---|---|---|---|---|---|---|
| Region/Method | 1 | 2 | 3 | 1 | 2 | 3 |
| Globe | −0.635 | −0.605 | −0.545 | −1.723*** | −1.650*** | −1.503*** |
| | [0.991] | [0.990] | [0.988] | [0.000] | [0.000] | [0.000] |
| Europe | −1.227 | −1.183 | −1.096 | −0.326 | −0.330 | −0.337 |
| | [0.966] | [0.967] | [0.969] | [0.257] | [0.246] | [0.223] |
| Asia | −0.727 | −0.672 | −0.562 | −2.873*** | −2.763*** | −2.542*** |
| | [0.859] | [0.850] | [0.828] | [0.000] | [0.000] | [0.000] |
| North America | 0.147 | 0.142 | 0.133 | −2.062*** | −1.981*** | −1.820*** |
| | [0.364] | [0.362] | [0.357] | [0.001] | [0.001] | [0.001] |
| South America | 0.198** | 0.190** | 0.175** | 0.401 | 0.388 | 0.362 |
| | [0.036] | [0.036] | [0.036] | [0.684] | [0.685] | [0.687] |
| Africa | 0.063 | 0.064 | 0.066 | 0.030** | 0.031** | 0.033** |
| | [0.309] | [0.297] | [0.268] | [0.030] | [0.031] | [0.033] |
| Australia | 0.493*** | 0.465*** | 0.410*** | 0.559 | 0.533 | 0.479 |
| | [0.001] | [0.001] | [0.001] | [0.990] | [0.990] | [0.990] |
| Arctic Circle | -0.046 | -0.048 | -0.050 | -0.065 | -0.058 | -0.044 |
| | [0.574] | [0.579] | [0.590] | [0.447] | [0.451] | [0.459] |
| Antarctica | 0.092 | 0.081 | 0.060 | −1.326** | −1.217** | −1.000** |
| | [0.284] | [0.291] | [0.310] | [0.010] | [0.010] | [0.009] |

Note: P-values of the one-sided tests for the reaction hypotheses obtained from HAC robust standard errors are in square brackets; $*$, $**$, $***$ denote statistical significance at 10%, 5% and 1% significance levels, respectively. The left panel considers the hypothesis $H_{0RL} : \lambda^L \leq 0$ against $H_{ARL} : \lambda^L > 0$ for the slope coefficient of the regression equation (4). The right panel considers the hypothesis $H_{0RR} : \lambda^R \geq 0$ against $H_{ARR} : \lambda^R < 0$ for the slope coefficient of the regression equation (5). Method 1 is the small-sample correction of the Hill estimator using demeaned data; Method 2 is the small-sample correction of the generalized least square estimator proposed in Aban and Meerschaert (2004), and Method 3 is the correction of the least squares estimator obtained in Tripathi (2014). The time series of estimates of $\xi$ are obtained from cross-sections of monthly temperatures recorded for each region and year over the period 1960 to 2022.

location-invariant approach for estimation, we contribute to improving our understanding of extreme temperature behavior. The findings from a thorough simulation study underscore the importance of considering both data characteristics and distributional properties when selecting suitable estimation methods. The application of the proposed methodology to real world temperature data from 1960 to 2022 provides empirical evidence supporting the existence of diverse extreme warming patterns across regions, with implications for policy decisions and climate change mitigation strategies.

Moreover, our proposed identification of specific tail effects beyond the expected shifts in mean temperatures enriches the understanding of extreme temperature dynamics and highlights the need for nuanced approaches to modeling climate change impacts. This study thus provides valuable insights for future research and policy development aimed at addressing the multifaceted challenges of climate change.

## References


Aban, I.B., and M.M. Meerschaert (2001). "Shifted Hill's estimator for heavy tails." *Communications in Statistics. Simulation Comput.* 30, 949–962.

Aban, I.B., and M.M. Meerschaert (2004). "Generalized least-squares estimators for the thickness of heavy tails." *Journal of Statistical Planning and Inference* 119, 341-352.

Adams, R. M., C. Rosenzweig, R. M. Peart, J. Ritchie, J. To, B. A. McCarl, J.D. Glyer, R.B. Curry, J.W. Jones, K.J. Boote, and L.H. Jr. Allen (1990). "Global Climate Change and US Agriculture." *Nature* 345, 219-224.

Andrews, D. W. K. (1991). "Heteroskedasticity and Autocorrelation Consistent Covariance Matrix Estimation." *Econometrica* 59, 817-858.

Ballester, J., Giorgi, F. and X. Rodó. (2010). "Changes in European temperature extremes can be predicted from changes in PDF central statistics. A letter." *Climatic Change* 98, 277–284.

Beaulieu, C., Gallagher, C., Killick, R., Lund, R, Shi, X. 2024. A recent surge in global warming is not detectable yet. *Communications earth & environment* 5:576.

Beirlant, J., P. Vynckier, and J.L. Teugels (1996). "Tail estimation, Pareto quantile plots, and regression diagnostics." *Journal of the American Statistical Association* 91, 1659–1667.

Chang, Y., Kim, Ch.S., and J.Y. Park (2016). "Nonstationarity in time series of state densities." *Journal of Econometrics* 192, 152-167.

Coles, S. (2001). An Introduction to Statistical Modeling of Extreme Values. Springer, London, ISBN:1-85233-459-2.

Danielsson, J., D.W. Jansen, and C.G. De vries (1996). "The method of moments ratio estimator for the tail shape parameter." *Communications in Statistics - Theory and Methods* 25 (4), 711-720.

de Haan, L. (1976). Sample extremes: an elementary introduction. *Statistica Neerlandica* 30 (4), 161-172.

Dekkers, A.L.M., J.H.J. Einmahl, and L. de Haan (1989). "A Moment estimator for the index of an extreme-value distribution." *The Annals of Statistics* 17 (4), 1833-1855.

Drees (1995). "Refined Pickands estimators of the extreme value index." *The Annals of Statistics* 23 (6), 2059-2080.

Easterling, D.R., Meehl, G., Changnon, S. ,Parmesan,C., Karl, T.R., and L.O. Mearns (2000). "Climate extremes: observations, modeling, and impacts." *Science* 289, 2068–2074.

Easterling, D.R., .Kunkel, K.E., Wehner, M.F. and L. Sun (2016). "Detection and attribution of climate extremes in the observed record." *Weather and Climate Extremes* 11, 17–27

Embrechts, P., C. Klüppelberg, and T. Mikosch (1997). Modelling Extremal Events for Insurance and Finance. New York: Springer.

Estrada, F., Perron, P., 2017. Extracting and analyzing the warming trend in global and hemispheric temperatures. *Journal of Time Series Analysis* 38, 711–732.

Fedotenkov, I. (2018). A review of more than one hundred Pareto-tail index estimators. Munich Personal RePEc Archive. Paper No. 90072. Available at *https://mpra.ub.uni-muenchen.de/90072*

Fraga Alves, M. I. (2001). "A location invariant Hill-type estimator." *Extremes* 4(3), 199-217.

Gabaix, X. (1999). "Zipf's Law for Cities: An Explanation." *Quarterly Journal of Economics* 114, 739-767.

Gabaix, X., and Y. Ioannides (2004). The Evolution of City Size Distributions. In *Handbook of Regional and Urban Economics* Vol. 4, eds. V. Henderson and J.-F. Thisse, Amsterdam: Elsevier North-Holland, 2341-2378.

Gabaix, X., and R. Ibragimov (2012). "Rank -1/2: A Simple Way to Improve the OLS Estimation of Tail Exponents." *Journal of Business and Economic Statistics* 29 (1), 24-39.

Gadea-Rivas, M.D., and J. Gonzalo (2020). Trends in distributional characteristics: Existence of global warming. *Journal of Econometrics* 214, 153-174.

Gadea-Rivas, M.D., and J. Gonzalo (2025). Climate change heterogeneity: A new quantitative approach. *Plos One,* January 2025.

Gnedenko, B.V. (1943). "Sur la distribution limite du terme maximum d'une serie aleatoire." *Annals of Mathematics* 44 (3), 423-453.

Gonzalo, J., and J. Olmo (2004). "Which extreme values are really extreme." Journal of Financial Econometrics 2, 3, 349-369.

Gumbel, E. J. (1941) "The return period of flood flows." *Annals of Mathematical Statistics* 12, 163-190.

Gumbel, E. J. (1958). Statistics of Extremes. Columbia University Press.

Hansen, J. and S. Lebedeff (1987). "Global Trends of Measured Surface Air Temperature." *Journal of Geophysics* 92, 13345-13372.

Hansen, J. and S. Lebedeff (1988). "Global Surface Air Temperature: Update through 1987." *Geophysical Res. Letters* 15, 323-326.

Hill, B. (1975). "A simple general approach to inference about the tail of a distribution." *Annals of Statistics* 3, 1163–1173.

Hsing, T. (1993). "Extremal index estimation for a weakly dependent stationary sequence." *The Annals of Statistics* 21(4), 2043-2071.

Jones P.D., D.H. Lister, T.J. Osborn, C. Harpham, M. Salmon, and C.P. Morice (2012). "Hemispheric and large-scale land surface air temperature variations: an extensive revision and an update to 2010." *Journal of Geophysical Research* 117, 1-29.

Huisman, R., K.G. Koedijk, C.J.M. Kool, and F. Palm (2001). "Tail-Index Estimates in Small Samples." *Journal of Business and Economic Statistics* 19 (2), 208-216.

IPCC, (2021). Climate Change 2021: The Physical Science Basis. Contribution of Working Group I to the Sixth Assessment Report of the Intergovernmental Panel on Climate Change[Masson-Delmotte, V., P. Zhai, A. Pirani, S.L. Connors, C. Pean, S. Berger, N. Caud, Y. Chen, L. Goldfarb, M.I. Gomis, M. Huang, K. Leitzell, E. Lonnoy, J.B.R. Matthews, T.K. Maycock, T. Waterfield, O. Yelek¸R. Yu, and B. Zhou (eds.)]. Cambridge University Press, Cambridge, 2021; United Kingdom and New York, NY, USA.

IPCC, (2022a). Climate Change 2022: Impacts, Adaptation, and Vulnerability. Contribution of Working Group II to the Sixth Assessment Report of the Intergovernmental Panel on Climate Change [H.-O. Pörtner, D.C. Roberts, M. Tignor, E.S. Poloczanska, K. Mintenbeck, A. Alegría, M. Craig, S. Langsdorf, S. Löschke, V. Möller, A. Okem, B. Rama (eds.). Cambridge University Press. In Press.

IPCC, (2022b). Climate Change 2022: Mitigation of Climate Change. Contribution of Working Group III to the Sixth Assessment Report of the Intergovernmental Panel on Climate Change [P.R. Shukla, J. Skea, R. Slade, A. Al Khourdajie, R. van Diemen, D. McCollum, M. Pathak, S. Some, P. Vyas, R. Fradera, M. Belkacemi, A. Hasija, G. Lisboa, S. Luz, J. Malley, (eds.)]. Cambridge University Press, Cambridge, 2022; United Kingdom and New York, NY, USA.

Katz, R.W., and B.G. Brown (1992). "Extreme events in a changing climate: variability is more important than averages." *Climatic Change* 21, 289-302.

Katz, R.W., Parlange M.B., and P. Naveau (2002) "Statistics of extremes in hydrology." *Adv Water Resources* 25, 1287-1304.

Katz, R.W. (2010). "Statistics of extremes in climate change." *Climatic Change* 100, 71–76.

Kennedy, J. J., Rayner, N. A., Atkinson, C. P. and Killick, R. E., 2019: An ensemble data set of sea-surface temperature change from 1850: the Met Office Hadley Centre HadSST.4.0.0.0 data set. Journal of Geophysical Research: Atmospheres 124, 7719-7763. https://doi.org/10.1029/2018JD029867.

Kratz, M. F., and S. Resnick (1996). "The qq-estimator and heavy tails." *Communications in Statistics. Stochastic Models* 12, 699–724.

Leadbetter, M.R., G. Lindgren, and H. Rootzén (1983). Extremes and Related Properties of Random Sequences and Processes. Springer, New York.

Ling, C., Peng, Z., S. Nadarajah (2007a). "A location invariant Moment-type estimator I." *Theory Probab. Math. Stat.* 76, 23–31 (2007a)

Ling, C., Peng, Z., S. Nadarajah (2007b). "A location invariant Moment-type estimator II." *Theory Probab. Math. Stat.* 77, 177–189 (2007b)

Ling, C., Peng, Z., and S. Nadarajah (2012). "Location invariant Weiss-Hill estimator." *Extremes* 15, 197-230.

Mearns, L.O., R.W. Katz, and S.H. Schneider (1984). "Extreme High-Temperature Events: Changes in their Probabilities with Changes in Mean Temperature." *Journal of Clim. Appl. Meteorol.* 23, 1601-1613.

Mitchell, J. E B., S. Manabe, V. Meleshko, and T. Tokioka (1990). Equilibrium Climate Change - and its Implications for the Future. In J. T. Houghton, G. J. Jenkins, and J. J. Ephranms (eds.), Climate Change: The IPCC Scientific Assessment. Cambridge University Press, Cambridge, pp. 131 - 172.

Newey, W. K., and K. D. West. (1987). "A Simple, Positive-Definite, Heteroskedasticity and Autocorrelation Consistent Covariance Matrix." *Econometrica* 55, 703-708.

Nicolau, J. and P.M. Rodrigues (2019). "A New Regression-Based Tail Index Estimator." *The Review of Economics and Statistics* 101 (4), 667-680.

O'Brien, G.L. (1987). "Extreme values for stationary and markov sequences." *The Annals of Probability* 15(1), 281-291.

Osborn, T.J., Jones, P.D., Lister, D.H., Morice, C.P., Simpson, I.R., Winn, J.P., Hogan, E., and Harris, I.C., 2021. Land surface air temperature variations across the globe updated to 2019: the CRUTEM5 dataset. Journal of Geophysical Research: Atmospheres. 126, e2019JD032352.

Park, J.Y., and J. Qian (2012). "Functional regression of continuous state distributions." *Journal of Econometrics* 167, 397-412.

Pickands III, J. (1975)." Statistical Inference Using Extreme Order Statistics." *The Annals of Statistics* 3, 119-131.

Rosen, K. T., and M. Resnick (1980). "The Size Distribution of Cities: An Examination of the Pareto Law and Primacy." *Journal of Urban Economics* 8, 165-186.

Seneviratne, S., Nichols, N., Easterling, D., Goodess, C., Kanae, S., Kossin, J., Luo,Y., Marengo, J., McInnes, K., Rahimi, M., Reichstein, M., Sorteberg, A., Vera,C., Zhang, X. (2012). Changes in climate extremes and their impacts on the natural physical environment, Chapter3 in IPCC Special Report on Managing the Risks of Extreme Events and Disasters to Advance Climate Change Adaptation. Cambridge University Press, Cambridge, UK, NewYork, NY,USA.

Tripathi, Y. M., S. Kumar, and C. Petropoulos (2014). "Improved estimators for parameters of a Pareto distribution with a restricted scale." *Statistical Methodology* 18, 1–13.

von Mises, R. (1936). "La distribution de la plus grande de n valeurs." *Rev. Math. Union Interbalcanique* 1, 141-160.

Wigley, T. M. L.. (1985). "Impact of Extreme Events." *Nature* 316, 106-107.

Wigley, T. M. L. (1988). "The Effect of Changing Climate on the Frequency of Absolute Extreme Events." *Climate Monitor* 17, 44-55.

Zwiers, F.W., Zhang,X. and Y. Feng, (2011). "Anthropogenic influence on long return period daily temperature extremes at regional scales." *Journal of Climate* 24, 881–892.

## Disclosure statement

The authors report no conflict of personal or financial interest.